ORIGINAL PAPER

ZAMM

A beam contact benchmark with analytic solution

Armin Bosten[1,2] | **Vincent Denoël**[1] | **Alejandro Cosimo**[1] | **Joachim Linn**[2] |
Olivier Brüls[1]

[1]University of Liège, Liege, Belgium

[2]Fraunhofer Institute for Industrial Mathematics, Kaiserslautern, Germany

Correspondence
Armin Bosten, University of Liège, Liege, Belgium.
Email: a.bosten@uliege.be

This paper presents a test case to help validate simulation codes for contact problems involving beams. A closed form solution is derived and the comparison is made with a finite element (FE) implementation that uses the mortar method for enforcing the contact constraints. The test case consists of a semi-infinite cantilever beam subjected to a constant distributed load and experiencing frictionless contact with a straight rigid substrate. Both an Euler-Bernoulli and a Timoshenko beam model are considered and the influence of the differing kinematic hypotheses is analyzed. In the case of the Euler-Bernoulli beam the distributed contact force is equal to the load along the contact region except at the boundary where a point load appears. On the contrary, the rigid substrate exerts a fully distributed load on the Timoshenko beam which decays exponentially from the first contact point and tends towards the applied load. The rate of decay depends on the relative shear deformability. Moreover, whereas in the first case the transverse shear force is discontinuous, it becomes continuous when allowing for shear deformation. An example of benchmarking is given for a particular FE code. The error with respect to the exact solution can be computed and it is shown that the numerical solution converges to the analytic solution when the FE mesh is refined.

1 | INTRODUCTION

In recent years interest in the modeling of systems with flexible slender structures experiencing contact interactions has grown significantly. Areas of application include the automotive, drilling, textile and medical industry. (The European project THREAD [1] investigates novel approaches to model and simulate slender, highly flexible beam-like structures for a broad variety of industrial applications.) In the majority of cases, numerical approaches, such as the Finite Element (FE) method, are chosen to model such systems [2–4]. These approaches are very versatile, however, they may not offer physical insight on the influence of the modeling parameters and assumptions when employed systematically. From that point of view, analytic approaches are highly valuable. Moreover, numerical schemes have to be validated by comparing them to a reference. Such validations may rely on analytic solutions to carefully designed, but simple test problems [5]. Therefore, the goal of this paper is to present a benchmark for simulation codes involving beam contact with a closed form analytic solution. The influence of certain parameters is studied and a comparison with a numerical method is made.

Different theories with varying complexity and physical accuracy are available to describe a beamlike structure. The fewer the kinematic assumptions, the closer a reduced model gets to the full 3D continuum model, but the more computationally expensive it is. Since in many numerical codes (with a few exceptions as in [3]), beam elements are based on Kirchhoff [6, 7] or Simo-Reissner [8–10] type beam theories, their linear two dimensional small displacement equivalents will be applied here. These are the shear free Euler-Bernoulli model and the Timoshenko model [11] that includes shearing. These models preclude deformation of cross sections.

Interestingly, the underlying (kinematic) assumptions have an influence on the solution of the contact problem. In the framework of a fully 3D continuum model cross sections locally deform to allow for continuous contact pressures. This continuity may only be obtained when transverse normal strain (i.e., deformability of cross sections) is included in the beam model [12, 13]. However, this level of detail is not always possible nor necessary when studying the overall behaviour of systems of components using a numerical approach. As mentioned before, in many cases beam models with undeformable cross sections are employed. In [14, 15], point and distributed contacts between the Euler elastica and rigid boundaries are studied. The distributed contact forces exhibit characteristic peaks or point loads at the boundaries of the contact regions. The introduction of shear deformation smoothes the problem to a certain extent and the contact force is fully distributed, but still discontinuous in that case. This is observed in [16], where the contact between a buckled Timoshenko beam and a rigid substrate is considered.

In this paper the focus is on a semi-infinite cantilever beam pressed onto a rigid wall by means of a constant distributed load. It can be seen as a free boundary problem, where the governing equations are solved analytically [17] or numerically [15, 18] on each subdomain that are defined by the limits of the contact region. Continuity equations are used to determine the location of this transition point. The solution we derive is simple and fully analytic. Parameters can be varied to make a benchmark for numerical methods based on Newton solution schemes without the use of continuation algorithms.

The paper is organized as follows. In Section 2, the problem under study is described and a dimensionless version of the equations is introduced. Closed form solutions for the Euler-Bernoulli and the Timoshenko case are derived in Section 3. In accordance with [16], we show that in the first case the distributed contact force is equal to the load along the contact region except at the boundary where a point load appears. On the contrary, the rigid substrate exerts a fully distributed load on the Timoshenko beam which decays exponentially from the first contact point and tends towards the applied load. The rate of decay depends on the relative shear deformability. Moreover, whereas in the first case the transverse shear force is discontinuous, it becomes continuous when allowing for shear deformation. Finally, in Section 4, an example of benchmarking is given for a FE implementation that uses the mortar method for enforcing the contact constraints. The computation of the numerical error is straightforward and any other numerical method could be validated using the solution developed in this paper. In particular, we observe that even though the numerical model has difficulties to capture the discontinuity of the contact forces at the boundary, optimal spatial convergence rates are obtained and the total integrated contact force approaches the analytical value from below under mesh refinement.

2 | PROBLEM STATEMENT AND DIMENSIONLESS FORMULATION

Figure 1 and shows a semi-infinite cantilever beam clamped at $x = 0$ and left free at the other end. It is subjected to a constant vertical distributed load p[N/m] and a contact reaction force $r(x)$[N/m]. The applied forces are counted positively in the upward direction. The vertical displacement is denoted by $w(x)$ and the initial gap by g[m]. They are taken positive in the downward direction. The beam enters in contact with the rigid substrate at $x = d$. The length of the free region, d, is a priori unknown. It separates the problem into two domains: the free region, where $x \in [0, d]$ and the contact region where $x \in [d, +\infty]$.

2.1 | Euler-Bernoulli model

In the linear, small displacement setting, the equation governing the Euler-Bernoulli beam [11] is

$$w''''(x) = \frac{p}{EI}, \tag{1}$$
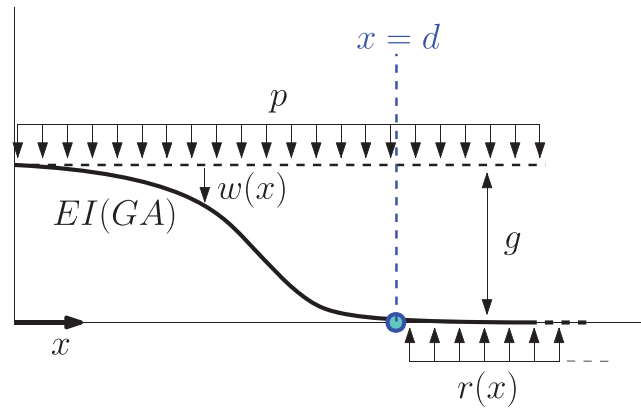
FIGURE 1   Dimensional variables.

where $EI[\text{Nm}^2]$ is the constant bending stiffness. It combines the equilibrium of the beam in the free region with a linear constitutive law. After solving Equation (1) the internal bending moment and the shear force are computed as

$$M(x) = -EIw''(x), \quad T(x) = -EIw'''(x). \tag{2}$$

In our conventions the internal bending moment is positive in the clockwise direction and the shear force in the vertical upward direction. Note that the equation for the shear force follows from the equilibrium of moments and thus only holds at equilibrium. Equation (1) needs to be solved in the free region, where the applied load is known. The boundary conditions at the clamp are $w(0) = w'(0) = 0$. We enforce continuity of the displacement and its slope at the transition point, that is $w(d) = g$ and $w'(d) = 0$, since the beam geometry is imposed by the rigid wall in the contact region. The length of the free region is obtained by imposing the continuity of the bending moment, $M(d) = 0$, since the bending moment in the contact region is zero.

2.2 | Timoshenko model

Under the same hypotheses as in the previous section, but allowing for shear deformation, the equations to be solved in the free region are [11]

$$w''''(x) = \frac{p}{EI}, \quad \theta'''(x) = \frac{p}{EI}, \quad w'(x) = \theta(x) - \frac{EI}{GA}\theta''(x), \tag{3}$$

where θ is the cross-section rotation angle and $GA[\text{N}]$ is the constant shear stiffness. The last equation is a kinematic condition that combines constitutive equations for the bending moment and the shear force with the equilibrium equations. The boundary conditions on the transverse displacement, $w(0) = w'(d) = 0$, $w(d) = g$, are complemented by $\theta(0) = 0$ at the fixed end and $\theta(d) = \theta_d$. The quantity θ_d was introduced to explicitly translate the continuity of the beam angle through the transition point. In the contact region, where $\bar{w}(x) = 0$, the governing equations are

$$\bar{\theta}'''(x) = \frac{p - r(x)}{EI}, \quad \bar{\theta}(x) - \frac{EI}{GA}\bar{\theta}''(x) = 0, \tag{4}$$

which have to be solved for θ and r together with the boundary conditions $\bar{\theta}(d) = \theta_d$ and $\bar{\theta} \to 0$ as $x \to +\infty$. A technical difference to the Euler-Bernoulli model concerning the solution approach is that a governing equation has to be solved in the contact region where not all kinematic quantities are trivially obtained. Notice that the overhead bar refers to variables in the contact region. As before, the extent d of the free region is determined by enforcing the continuity of the bending moment at $x = d$. The shear forces and bending moments at equilibrium are given by

$$M(x) = -EI\theta'(x), \quad T(x) = -EI\theta''(x), \quad \bar{M}(x) = -EI\bar{\theta}'(x), \quad \bar{T}(x) = -EI\bar{\theta}''(x), \tag{5}$$

in each region respectively.

2.3 | Dimensionless variables

The problem is characterized by the following two length scales

$$u_1^* = g, \quad u_2^* = \left(\frac{gEI}{p} \right)^{1/4}. \tag{6}$$

The first one is the initial gap. It is the maximal transverse deflection of the beam. The second one is a longitudinal lengthscale, which is a characteristic beam length with maximal transverse displacement g for given bending stiffness and applied load. Therefore, it is natural to scale the variables of the problem as $\xi = x/u_2^*$ and $\delta = d/u_2^*$. The dimensionless transverse displacement of the beam is defined as

$$\nu(\xi) = \frac{w[x(\xi)]}{u_1^*}. \tag{7}$$

The angle $\theta(x)$ is related to the slope $w'(x)$ of the neutral axis. It is thus naturally scaled by

$$\theta^* = \frac{u_1^*}{u_2^*} = \left(\frac{pg^3}{EI} \right)^{1/4} \tag{8}$$

such that the dimensionless angles

$$\vartheta(\xi) = \frac{\theta[x(\xi)]}{\theta^*}, \quad \bar{\vartheta}(\xi) = \frac{\bar{\theta}[x(\xi)]}{\theta^*} \tag{9}$$

are of order 1. The characteristic bending moment and shear force are chosen as $T^* = pu_2^*$ and $M^* = pu_2^{*2}$, such that the dimensionless analogue of Equation (2) is

$$\mathcal{M}(\xi) = \frac{M[x(\xi)]}{M^*} = -\nu''(\xi), \quad \mathcal{T}(\xi) = \frac{T[x(\xi)]}{T^*} = -\nu'''(\xi) \tag{10}$$

and for Equation (5) we get

$$\mathcal{M}(\xi) = -\vartheta'(\xi), \quad \mathcal{T}(\xi) = -\vartheta''(\xi), \quad \bar{\mathcal{M}}(\xi) = -\bar{\vartheta}'(\xi), \quad \bar{\mathcal{T}}(\xi) = -\bar{\vartheta}''(\xi). \tag{11}$$

In the Timoshenko model, the reaction $r(x)$ along the wall plays an important role. It is naturally scaled by p. Thus, we define its adimensional counterpart as $\rho(\xi) = r[x(\xi)]/p$. Finally, the dimensionless relative shear deformability of the Timoshenko beam will naturally appear as

$$\epsilon^2 = \frac{EI}{GAu_2^{*2}} = \frac{(EIgp^3)^{1/4}}{GA}. \tag{12}$$

An illustration of the problem with adimensional variables is given in Figure 2.

3 | ANALYTICAL SOLUTION

3.1 | Euler-Bernoulli model

Under the change of variables introduced in Section 2.3 the Euler-Bernoulli beam is governed by

$$\nu''''(\xi) = 1, \quad \xi \in [0, \delta] \tag{13}$$
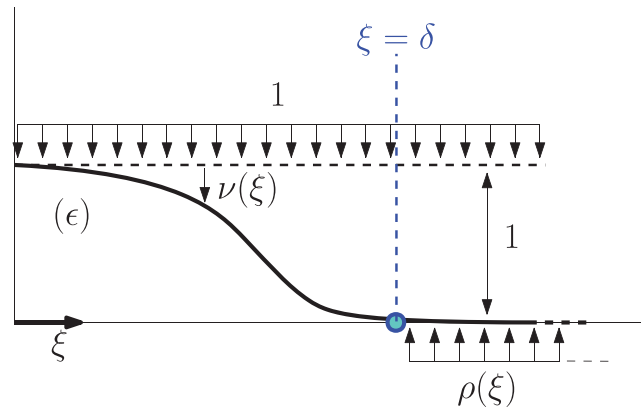
FIGURE 2 Dimensionless variables.

with $v(0) = v'(0) = v'(\delta) = 0, v(\delta) = 1$. The solution is

$$v(\xi) = \frac{\xi^4}{24} - \left(\frac{2}{\delta^3} + \frac{\delta}{12}\right)\xi^3 + \left(\frac{3}{\delta^2} + \frac{\delta^2}{24}\right)\xi^2. \tag{14}$$

The continuity of the bending moment yields $\delta = 72^{1/4}$. The dimensionless shear force has the following simple expression

$$\mathcal{T}(\xi) = -\xi + \delta\left(\frac{1}{2} + \frac{12}{\delta^4}\right). \tag{15}$$

such that at the boundaries one has

$$\mathcal{T}(0) = \frac{2}{3}\delta, \quad \mathcal{T}(\delta) = -\frac{1}{3}\delta. \tag{16}$$

Since $\bar{v}(\xi) = 1$ in the contact region, the shear force at the boundary is given by

$$\bar{\mathcal{T}}(\delta) = 0. \tag{17}$$

Unlike the bending moment, the shear force is thus discontinuous at $\xi = \delta$. As a consequence, the contact reaction includes a point load of magnitude

$$f_\delta = \bar{\mathcal{T}}(\delta) - \mathcal{T}(\delta) = \frac{1}{3}\delta. \tag{18}$$

Hence, one third of the distributed load applied to the beam in the free region ends up as a point contact reaction force at the contact boundary. The other two thirds are transmitted into the clamp. The distributed contact force in the region $\xi > \delta$ is simply $\rho(\xi) = 1$.

3.2 | Timoshenko model

Free region: After the change of variables Equation (3) become

$$v''''(\xi) = 1, \quad \vartheta'''(\xi) = 1, \quad v'(\xi) = \vartheta(\xi) - \epsilon^2\vartheta''(\xi) \tag{19}$$

and the boundary conditions are $v(0) = v'(\delta) = 0$, $v(\delta) = 1$ for the adimensional transverse displacement and $\vartheta(0) = 0$, $\vartheta(\delta) = \vartheta_\delta$ for the adimensional beam angle. From the first two equations and the clamping conditions one knows that

the deflection is of the form

$$v(\xi) = \frac{\delta^4}{24}\left(\left(\frac{\xi}{\delta}\right)^4 + A\left(\frac{\xi}{\delta}\right)^3 + B\left(\frac{\xi}{\delta}\right)^2 + C\left(\frac{\xi}{\delta}\right)\right), \tag{20}$$

and that the beam angle is of the form

$$\vartheta(\xi) = \frac{\delta^3}{6}\left(\left(\frac{\xi}{\delta}\right)^3 + D\left(\frac{\xi}{\delta}\right)^2 + E\left(\frac{\xi}{\delta}\right)\right). \tag{21}$$

The five constants A, B, C, D and E may be obtained using the two boundary conditions at the contact interface, together with the third equation in (19). These are

$$A = -2\Delta\left(1 + \frac{24}{\delta^4}\right), \tag{22a}$$

$$B = -\frac{3}{\delta}\left(1 + \frac{8}{\delta^3}\right) + 4\Delta\left(1 + \frac{24}{\delta^4}\right), \tag{22b}$$

$$C = -2\left(1 + \frac{24}{\delta^4}\right)(\Delta - 1), \tag{22c}$$

$$D = -\frac{3}{2}\Delta\left(1 + \frac{24}{\delta^4}\right), \tag{22d}$$

$$E = -\frac{5}{2} + \frac{1}{\Delta} + 2\Delta + \frac{12}{\delta^4}(4\Delta - 1), \tag{22e}$$

where we defined an additional adimensional parameter $\Delta = \frac{\delta^2}{\delta^2 + 6\epsilon^2}$. The shear force and the bending moment may now be computed

$$\mathcal{T}(\xi) = -\xi - \frac{\delta}{3}D, \quad \mathcal{M}(\xi) = -\frac{\xi^2}{2} - \frac{\delta}{3}D\xi - \frac{\delta^2}{6}E \tag{23}$$

Note that one can verify that $\mathcal{T}(0) - \mathcal{T}(\delta) = \delta$, such that vertical equilibrium is satisfied. Contact region: The adimensional equations are

$$\bar{\vartheta}'''(\xi) = 1 - \rho(\xi), \quad \bar{\vartheta}(\xi) - \epsilon^2\bar{\vartheta}''(\xi) = 0. \tag{24}$$

We start by solving the third equation for $\vartheta(\xi)$ together with the boundary conditions $\bar{\vartheta}(\delta) = \vartheta_\delta$ and $\bar{\vartheta} \to 0$ as $\xi \to +\infty$. The solution is given by

$$\bar{\vartheta}(\xi) = \vartheta_\delta e^{(\delta - \xi)/\epsilon}. \tag{25}$$

The internal bending moment and shear force in the contact region follow as

$$\bar{\mathcal{T}}(\xi) = -\frac{\vartheta_\delta}{\epsilon^2}e^{(\delta - \xi)/\epsilon}, \quad \bar{\mathcal{M}}(\xi) = \frac{\vartheta_\delta}{\epsilon}e^{(\delta - \xi)/\epsilon} \tag{26}$$

Finally, from the second equation in (24) the adimensional distributed contact force exerted on the beam is computed as

$$\rho(\xi) = \frac{\vartheta_\delta}{\epsilon^3}e^{(\delta - \xi)/\epsilon} - 1. \tag{27}$$

TABLE 1 Numerical values of the dimensional quantities used to generate all figures throughout the paper.

Parameter	Value	Unit
R	1	mm
g	0.01	mm
L	0.3	m
p	1	N/m
I	0.79	mm^4
E	200	GPa
A	3.1	mm^2
G_{ref}	77	GPa

The total contact reaction force over a region $\xi \in [\delta, \mathcal{L}]$ is

$$f_c = \int_\delta^{\mathcal{L}} \rho(\xi)\,d\xi = \frac{\vartheta_\delta}{\epsilon^2}\left(1 - e^{(\delta - \mathcal{L})/\epsilon}\right) + (\mathcal{L} - \delta). \tag{28}$$

Subtracting the constant part of the contact force and taking $\mathcal{L} \to \infty$ yields an equivalent contact force in the transition region which may be compared to the point force from the Euler-Bernoulli case in Equation (18). It is equal to

$$f_\delta = \frac{\vartheta_\delta}{\epsilon^2}. \tag{29}$$

For small ϵ, this resultant force is concentrated in a thin boundary layer of length ϵ and located close to the transition point [19].

Transition point:

The beam angle at the transition point is

$$\vartheta_\delta = \frac{\epsilon^2 \Delta}{2\delta^3}\left(\delta^4 + 12\delta^2\epsilon^2 - 24\right). \tag{30}$$

The continuity of the bending moment is used to derive the following equation for the adimensional free length

$$\delta^6 + 6\epsilon\delta^5 + 30\epsilon^2\delta^4 + 72\epsilon^3\delta^3 + 72(\epsilon^4 - 1)\delta^2 - 144\epsilon(\delta + \epsilon) = 0 \tag{31}$$

By Descartes' rule of signs the above equation has a unique positive solution. The value of δ from the Euler-Bernoulli model may be used as initial guess for an iterative solution procedure. Interestingly, it can be verified that $\mathcal{T}(\delta) - \bar{\mathcal{T}}(\delta) = 0$ and thus, unlike in the Euler-Bernoulli case, the shear force is continuous and no additional point load at the contact boundary appears.

Figure 3a shows the transverse displacement, bending moment and shear force for different values of the relative shear deformability ϵ. We can already observe that increasing ϵ shortens the length of the free region, which is bounded from above by its value taken in the Euler-Bernoulli case. For a better understanding of the magnitude of the quantities involved, realistic dimensional parameters were chosen. These are given in Table 1 and represent a thin circular steel rod. To judge the shear stiffness of the Timoshenko beam we may compute a slenderness ratio of the beam in the free region as $R/d_{Tym} = 0.0097$. Notice that L denotes the finite beam length considered in the numerical models, whereas $L \to \infty$ in the analytic case. We assume that boundary effects are negligible such that both solutions can be compared. The resulting reference value for the shear deformability is $\epsilon_{ref} = 0.023$. The value of ϵ is increased by choosing a larger shear stiffness G, while keeping all other parameters fixed. The same parameter set will be used for all remaining figures throughout the paper.

The distributed contact reaction force ρ for different values of the relative shear deformability, is represented in Figure 3b. It is also compared to the Euler-Bernoulli model. As ϵ decreases, the contact force gets more concentrated around the transition region and tends towards a point load. Indeed, one can show analytically that when ϵ becomes

negligible

$$\lim_{\epsilon \to 0} \rho(\delta) = +\infty. \tag{32}$$
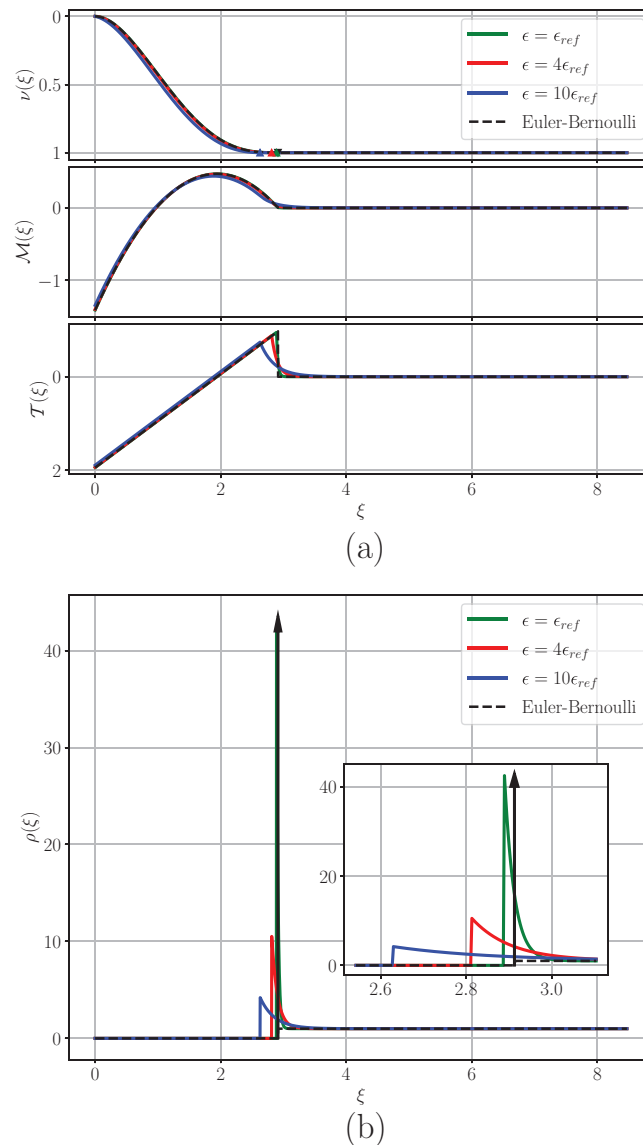
FIGURE 3 Illustration of the analytic solution. Comparison between the shear free case and different values of the relative shear deformability ϵ. (a) Transverse displacement, bending moment, shear force. The markers denote the first contact point. (b) Distributed contact force.

4 | COMPARISON WITH NUMERICAL MODELS

In this section the analytic solutions developed previously are compared to the FE implementation from [8, 20–22]. The beam model presented therein is a restating of the well known Simo-Reissner beam [23] on the special Euclidean group $SE(3)$. Unlike most formulations, the equilibrium equations are solved in the local frame attached to the cross-section and the discretization scheme couples translation and rotation variables. The mortar method is employed for obtaining a numerical solution to the contact problem. It consists in solving the contact constraint in a weak sense using a field of

Lagrangian multipliers that play the role of distributed contact force. The point-wise non-penetration constraint is replaced by a weighted integral that involves the basis functions of the Lagrangian multipliers.

The beam model presented in the aforementioned references includes shear deformation. For a consistent comparison with the analytical results from Section 3.1, we additionally introduce a Kirchhoff model that is based on the beam formulation on $SE(3)$. Shear deformation is prevented by means of constraints enforced via an augmented Lagrangian approach.

4.1 | Kirchhoff constraints and constraint gradient

The configuration of a two noded beam FE of length hu_2^*, where h is the adimensional element length, is given by $q = (\mathbf{H}_A, \mathbf{H}_B)$ with $\mathbf{H}_A, \mathbf{H}_B \in SE(3)$. The relative configuration between the two nodes A and B is given by

$$\widetilde{\mathbf{d}} = \log_{SE(3)}\left(\mathbf{H}_A^{-1}\mathbf{H}_B\right), \qquad \widetilde{\mathbf{d}} \in \mathfrak{se}(3). \tag{33}$$

The interpolated deformations in the FE are considered constant and therefore the vanishing shear constraint may simply be written as

$$\mathbf{g} = \mathbf{D}(\mathbf{d} - \mathbf{d}_0) = \mathbf{0}_{2\times 1}, \qquad \mathbf{d} \in \mathbb{R}^6, \tag{34}$$

where $\mathbf{D} = \begin{bmatrix} 0 & 1 & 0 & 0 & 0 & 0 \\ 0 & 0 & 1 & 0 & 0 & 0 \end{bmatrix}$ and $\mathbf{d}_0$ is the relative configuration vector in the reference configuration. The constraint gradient is computed as

$$\delta\mathbf{g} = \mathbf{D}\begin{bmatrix} -\mathbf{T}_{SE(3)}^{-1}(-\mathbf{d}) & \mathbf{T}_{SE(3)}^{-1}(\mathbf{d}) \end{bmatrix}\begin{bmatrix} \delta\boldsymbol{\pi}_A \\ \delta\boldsymbol{\pi}_B \end{bmatrix}, \qquad \widetilde{\delta\boldsymbol{\pi}}_A, \widetilde{\delta\boldsymbol{\pi}}_B \in \mathfrak{se}(3). \tag{35}$$

The operators involved in Equations (33) and (35) may be found in [8].

4.2 | Results and discussion

A good agreement between the exact and the numerically computed transverse displacement, v_h, is obtained for both beam models, as may be seen in Figure 4. This stays true for a small number of FEs, as shown by the discretization error in Figure 5a, which is defined as

$$e_d = \sqrt{\frac{\int_0^{\mathcal{L}} |v_h(\xi) - v(\xi)|^2 \, d\xi}{\int_0^{\mathcal{L}} v(\xi)^2 \, d\xi}}. \tag{36}$$

The spatial convergence rate of 2, characteristic for constant deformation elements, is conserved [21].

Since the mortar formulation assumes distributed contact forces and interpolates them, in this case with linear shape functions, the method cannot represent the point contact force that appears in the exact solution of the Euler-Bernoulli case. Similarly, the discontinuity followed by a potentially sharp gradient in the Timoshenko case induces oscillations in the interpolated contact force. Note that this does not affect the optimal spatial convergence rate. As may be seen in Figure 4, these oscillations may be reduced by mesh refinement. An important parameter is the ratio between the element length h and the characteristic length of the boundary layer, which is given by the relative shear deformability ϵ. When the latter is decreased, the peak in the distributed contact force is sharper, resulting in a problem with more numerical difficulties. Discretizations too coarse to represent the short spatial scales in the boundary layer, that is, such that $h > \epsilon$ (see Figure 4c), will result in a poor approximation of the distributed contact force. Outside this transition region, the distributed contact force is equal to the applied load and the numerical solution agrees with the exact one. Another
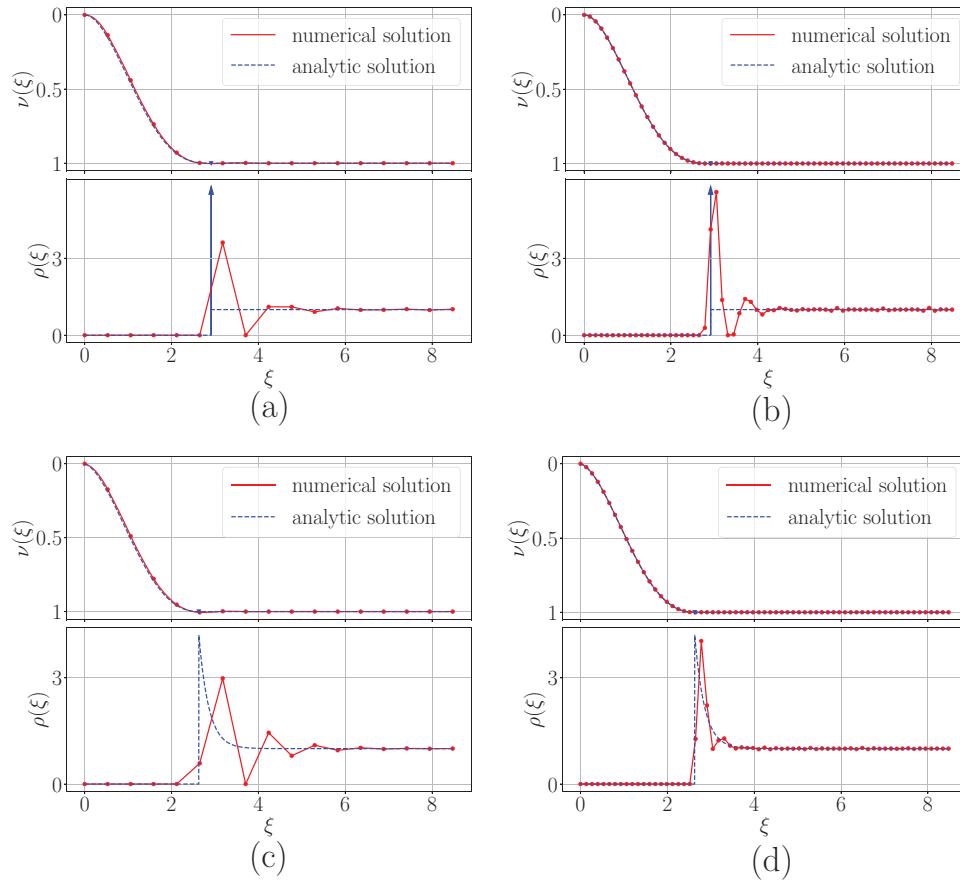
FIGURE 4 Comparison between analytic and numerical solutions of the transverse displacement and distributed contact reaction force for a coarse and a fine mesh. (a) Euler-Bernoulli with $h = 0.53$. (b) Euler-Bernoulli with $h = 0.13$. (c) Timoshenko with $\epsilon = 10\epsilon_{ref}$ and $h = 0.53 > \epsilon$. (d) Timoshenko with $\epsilon = 10\epsilon_{ref}$ and $h = 0.13 < \epsilon$.

interesting quantity to look at is the numerical resultant contact force acting on the beam and denoted f_{c_h}, obtained by integrating the distributed contact force along the contact region.

Figure 5b shows the relative error with respect to the analytic solution which is defined as

$$e_f = \frac{\left| f_{c_h} - f_c \right|}{f_c}. \tag{37}$$

As for the vertical deflection, we observe second order convergence. Figure 5c shows the evolution of the numerical free length δ_h as the mesh is refined. We take it as the average location of the first non-vanishing node and the maximum in the distributed contact force. The convergence behaviour is more uniform for larger values of the relative shear deformability.

5 | CONCLUSION

An analytic closed form solution for a clamped beam subjected to a constant distributed load and in contact with a rigid wall was derived. Both an Euler-Bernoulli and a Timoshenko Beam model were considered, and a static, small displacement setting was assumed. The problem may be set up as a numerical benchmark in a simple manner, without the need for continuation methods or dynamic simulation, since it does not involve any buckling. In this paper, the exact solution was compared to a FE implementation that uses the mortar method for enforcing the contact constraint. The main conclusions are the following:
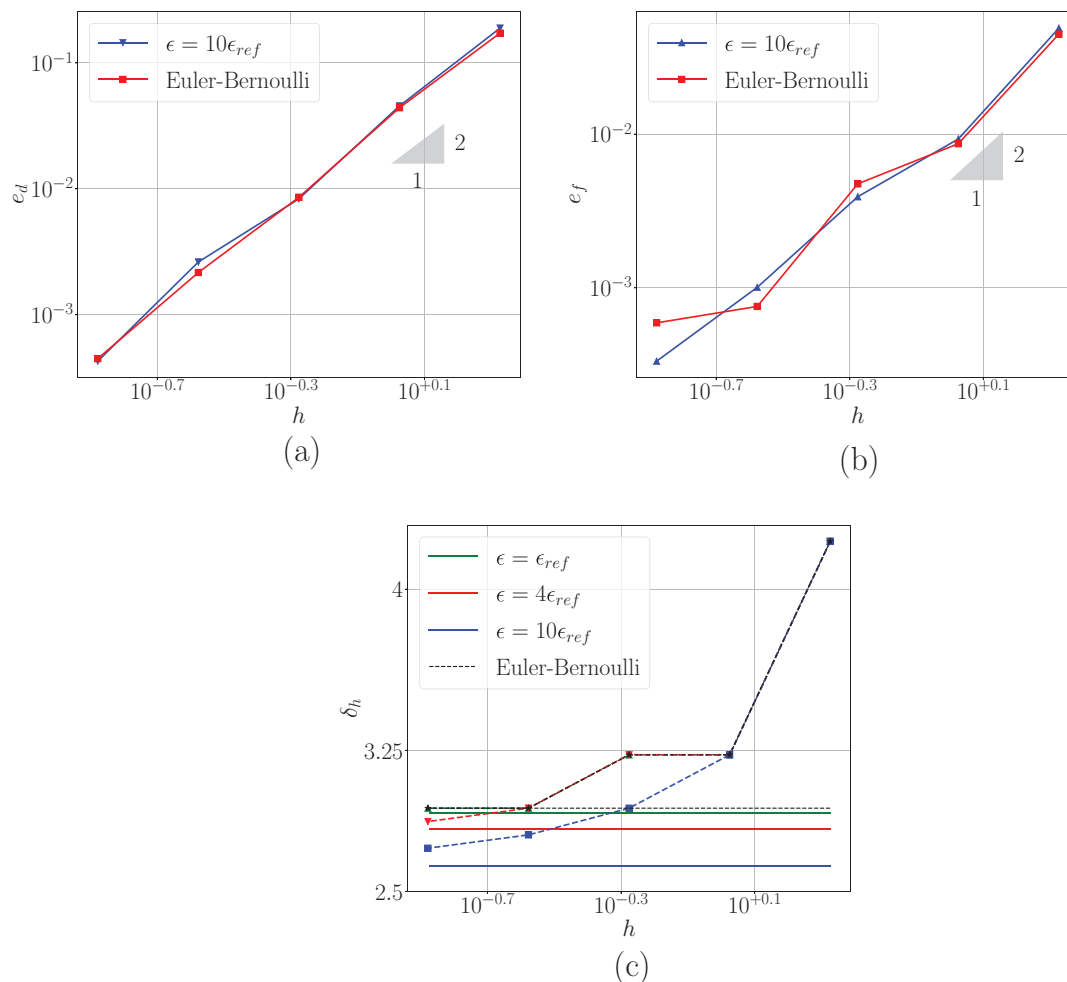
FIGURE 5 Convergence analysis for different quantities of interest. The horizontal lines represent the analytic value. (a) Error on the vertical displacement. (b) Error on the integrated contact force. (c) Length of the free region.

1. The Euler-Bernoulli model leads to a point contact force at the boundary of the contact region and the shear force is discontinuous. For the Timoshenko beam however, a purely distributed load is exerted by the wall, and the shear force is continuous. The observed spike in the distributed contact force increases when the shear deflection decreases, such that the solution for the Timoshenko model tends towards the solution of the Euler-Bernoulli model.

2. The discontinuity and high intensity of the contact forces at the contact boundary are difficult to be captured by a numerical model, since they occur over extremely short spatial scales. Indeed, the typical size of these short boundary layers is ϵ in the Timoshenko model and 0 in the Euler-Bernoulli model. As was shown in other works, these local effects are a consequence of the selected kinematic hypothesis of the underlying beam model and would not occur if a 3D continuum model of the beam was adopted. Generally, such local effects are of no importance to multibody system simulations, where reduced beam models, as they were studied here, are often employed. For such applications, the interest lies in the overall behaviour of assemblies of components. From that point of view, the mortar approach provides a reasonable approximation of the distributed contact forces. Indeed, the optimal spatial convergence rates are not affected.

ACKNOWLEDGEMENTS

REFERENCES

[1] Arnold, M., Brüls, O., Linn, J.: THREAD-numerical modeling of highly flexible structures for industrial applications. In: Celledoni, E., Münch, A. (eds.) Mathematics with Industry: Driving Innovation-ECMI Annual Report 20A9, pp. 20–25 (2019)

[2] Meier, C., Grill, M.J., Wall, W.A., Popp, A.: Geometrically exact beam elements and smooth contact schemes for the modeling of fiber-based materials and structures. Int. J. Solids Struct. 154, 124–146 (2018)

[3] Durville, D.: Contact-friction modeling within elastic beam assemblies: an application to knot tightening. Comput. Mech. 49, 687–707 (2012)

[4] Daviet, G., Bertails-Descoubes, F., Boissieux, L.: A hybrid iterative solver for robustly capturing coulomb friction in hair dynamics. ACM T. Graphic. Proc. of SIGGRAPH Asia. 30, 1–12 (2011)

[5] Konyukhov, A., Shala, S.: New benchmark problems for verification of the curve-to-surface contact algorithm based on the generalized Euler-Eytelwein problem. Numer. Meth. Engrg. 123, 411–443 (2022)

[6] Bertails, F., Audoly, B., Cani, M.-P., Querleux, B., Leroy, F., Lévêque, J.-L.: Super-helices for predicting the dynamics of natural hair. ACM Trans. Graph. 25, 1180–1187 (2006)

[7] Meier, C., Popp, A., Wall, W.A.: An objective 3D large deformation finite element formulation for geometrically exact curved Kirchhoff rods. Comput. Methods Appl. Mech. Eng. 278, 445–478 (2014)

[8] Sonneville, V., Cardona, A., Brüls, O.: Geometrically exact beam finite element formulated on the special Euclidean group SE (3). Comput. Methods Appl. Mech. Engrg. 268, 451–474 (2014)

[9] Cottenceau, E., Thomas, O., Véron, P., Alochet, M., Deligny, R.: Finite Elem. Anal. Dis. 139, 14 (2018)

[10] Lang, H., Linn, J., Arnold M.,: Multi-body dynamics simulation of geometrically exact Cosserat rods. Multibody Syst. Dyn. 25, 285–312 (2011)

[11] Géradin, M., Rixen, D.: Mechanical Vibrations: Theory and Application to Structural Dynamics. Wiley and Sons, Chichester, UK (2015)

[12] Essenburg, F.: On the significance of the inclusion of the effect of transverse normal strain in problems involving beams with surface constraints. ASME J. Appl. Mech. 42, 127–132 (1975)

[13] Naghdi, P.M., Rubin, M.B.: On the significance of normal cross-sectional extension in beam theory with application to contact problems. Int. J. Solids Struct. 25, 249–265 (1989)

[14] Soong, T.C., Choi, I.: An elastica that involves continuous and multiple discrete contacts with a boundary. Int. J. Mech. Scs. 28, 1–10 (1986)

[15] Denoël, V., Detournay, E.: Eulerian formulation of constrained elastica. Int. J. Sol. Struct. 48, 625–636 (2011)

[16] Chen, J.-S.: On the contact behavior of a buckled Timoshenko beam constrained laterally by a plane wall. Acta Mech. 222, 225–232 (2011)

[17] Denoël, V.: Advantages of a semi-analytical approach for the analysis of an evolving structure with contacts. Commun. Numer. Meth. Engng. 24, 1667-1683 (2008)

[18] Huynen, A., Detournay, E., Denoël, V.: Eulerian formulation of elastic rods. Proc. R. Soc. A 472 (2016)

[19] Hinch, E.J.: Perturbation Methods, p. 160. Cambridge University Press, (1991)

[20] Sonneville, V., Brüls, O., Bauchau, O.: Interpolation schemes for geometrically exact beams: a motion approach. Int. J. Numer. Methods Eng. 112, 1129–1153 (2017)

[21] Bosten, A., Cosimo, A., Linn, J., Brüls, O.: A mortar formulation for frictionless line-to-line beam contact. Multibody Syst. Dyn. 54, 31–52 (2021)

[22] Tomec, J., Jelenić, G.: Analysis of static frictionless beam-to-beam contact using mortar method. Multibody Syst. Dyn. 55, 293–322 (2022)

[23] Simo, J.C.: A finite strain beam formulation. The three-dimensional dynamic problem. Part I. Comput. Methods Appl. Mech. Eng. 49, 55–70 (1985)